

# Online Research @ Cardiff

This is an Open Access document downloaded from ORCA, Cardiff University's institutional repository: <http://orca.cf.ac.uk/100346/>

This is the author's version of a work that was submitted to / accepted for publication.

Citation for final published version:

Catar, Rusan, Witowski, Janusz, Zhu, Nan, Lücht, Christian, Derrac Soria, Alicia, Uceda Fernandez, Javier, Chen, Lei, Jones, Simon, Fielding, Ceri A., Rudolf, Andras, Topley, Nicholas, Dragun, Duska and Jörres, Achim 2017. IL-6 trans-signaling links inflammation with angiogenesis in the peritoneal membrane. *Journal of the American Society of Nephrology* 28 (4) , pp. 1188-1199. 10.1681/ASN.2015101169 file

Publishers page: <http://dx.doi.org/10.1681/ASN.2015101169>  
<<http://dx.doi.org/10.1681/ASN.2015101169>>

Please note:

Changes made as a result of publishing processes such as copy-editing, formatting and page numbers may not be reflected in this version. For the definitive version of this publication, please refer to the published source. You are advised to consult the publisher's version if you wish to cite this paper.

This version is being made available in accordance with publisher policies. See <http://orca.cf.ac.uk/policies.html> for usage policies. Copyright and moral rights for publications made available in ORCA are retained by the copyright holders.



## IL-6 trans-signaling links inflammation with angiogenesis in the peritoneal membrane

Rusan Catar <sup>1,\*</sup>, Janusz Witowski <sup>1,2,\*</sup>, Nan Zhu <sup>1</sup>, Christian Lücht <sup>1</sup>, Alicia Derrac Soria <sup>3</sup>, Javier Uceda Fernandez <sup>3</sup>, Lei Chen <sup>1</sup>, Simon A. Jones <sup>3</sup>, Ceri A. Fielding <sup>3</sup>, Andras Rudolf <sup>2</sup>, Nicholas Topley <sup>3,4</sup>, Duska Dragun <sup>1</sup>, Achim Jörres <sup>1,5</sup>

<sup>1</sup> Department of Nephrology and Medical Intensive Care, Charité-Universitätsmedizin Berlin, Campus Virchow-Klinikum, Berlin, Germany;

<sup>2</sup> Department of Pathophysiology, Poznan University of Medical Sciences, Poznań, Poland;

<sup>3</sup> Division of Infection and Immunity, The School of Medicine, Cardiff University, Heath Campus, Cardiff, UK.

<sup>4</sup> Wales Kidney Research Unit, The School of Medicine, Cardiff University, Heath Campus, Cardiff, UK.

<sup>5</sup> Department of Medicine I - Nephrology, Transplantation & Medical Intensive Care, University Witten/Herdecke, Medical Center Cologne-Merheim, Cologne, Germany

\* R.C. and J.W. contributed equally to this study

### Running title:

IL-6 trans-signaling induces VEGF

**Word count** (abstract): 213

**Word count** (main text, excl. title page, methods, figure legends, tables, references): XXXX

**Correspondence:**

Professor Achim Jörres; Department of Medicine I - Nephrology, Transplantation & Medical Intensive Care, University Witten/Herdecke, Medical Center Cologne-Merheim, Ostmerheimer Str. 2000, D-51109 Cologne, Germany; E-mail: [JoerresA@kliniken-koeln.de](mailto:JoerresA@kliniken-koeln.de)

## ABSTRACT

Vascular endothelial growth factor (VEGF) is implicated in peritoneal membrane remodeling that limits ultrafiltration in peritoneal dialysis (PD). While the exact mechanism of VEGF induction in PD is unclear, VEGF concentrations in drained dialysate correlate with IL-6 levels suggesting a link between these cytokines. Human peritoneal mesothelial cells (HPMC), the main source of IL-6 and VEGF in the peritoneum, do not bear cognate IL-6 receptor and are thus unable to respond to classical IL-6 receptor signaling. Here, we show VEGF release by HPMC is controlled by IL-6 in combination with its soluble receptor (IL-6 trans-signaling). Although IL-6 and soluble IL-6 receptor (sIL-6R) alone had no effect on VEGF production, stimulation of HPMC with IL-6 in combination with sIL-6R promoted VEGF expression through a transcriptional mechanism involving STAT3 and SP4. Induction of VEGF was functionally active and conditioned medium from HPMC cultured with IL-6 and sIL-6R promoted angiogenic endothelial tube formation, which could be blocked by silencing SP4. To verify these *in vitro* observations, induction of peritoneal inflammation in wild type and IL-6-deficient mice further demonstrated IL-6 involvement in the control of SP4, **VEGF and new vessel formation**, confirming the role for IL-6 trans-signaling in these processes. Taken together these findings identify a novel mechanism linking IL-6 trans-signalling and angiogenesis in the peritoneal membrane.

## INTRODUCTION

The efficacy of peritoneal dialysis (PD) as a treatment modality largely depends on the peritoneal membrane integrity. Dysfunction of the peritoneum as a dialysis organ may result from progressive membrane injury occurring over time on PD. The underlying pathophysiological mechanisms involve a gradual rise in small solute transport due to an increase in peritoneal perfusion and a decrease in peritoneal hydraulic conductance due to tissue fibrosis.<sup>1</sup> Both these processes are related to peritoneal angiogenesis. On the one hand, an increase in peritoneal vascularity increases the surface area available for solute diffusion and leads to rapid dissipation of the osmotic gradient that drives ultrafiltration. On the other hand, angiogenesis is a prominent feature of tissue repair, scar formation and fibrosis. Indeed, it has been estimated that up to 75% of patients with ultrafiltration failure may have increased vascular surface area.<sup>2;3</sup> Moreover, peritoneal biopsies taken from PD patients show that fibrosis occurs significantly more often in the presence of vasculopathy,<sup>4</sup> and the density of peritoneal blood vessels and sub-mesothelial and perivascular fibrosis are significantly greater in patients with membrane failure.<sup>4-6</sup> Animal models of PD confirm the existence of an inverse correlation between increased vascularization and ultrafiltration.<sup>7</sup> These studies suggest that a decline in ultrafiltration could be partially abrogated by anti-angiogenic therapy.<sup>7</sup>

Vascular endothelial growth factor (VEGF) is the most important pro-angiogenic mediator.<sup>8</sup> The impact of VEGF on peritoneal vascularity is demonstrated by the association of genetic polymorphisms determining increased VEGF production with increased peritoneal solute transport.<sup>9</sup> Moreover, the rates of VEGF appearance in the dialysate are elevated in patients with high peritoneal transport status.<sup>10;11</sup>

Several mechanisms are implicated in peritoneal VEGF induction in PD.<sup>12</sup> One of the factors involved has been suspected to be interleukin-6 (IL-6), since IL-6 concentrations in the drained dialysate correlate with peritoneal solute transport rates<sup>13-15</sup> and dialysate levels of VEGF.<sup>10;14</sup> Interestingly, it has been demonstrated that the peritoneal mesothelium is the main source of both VEGF<sup>16;17</sup> and IL-6.<sup>18;19</sup> Although VEGF can be induced by several inflammatory cytokines<sup>20</sup>, IL-6 has not been classically viewed as a driver of VEGF production in mesothelial cells, as these do not express the cognate IL-6 receptor (IL-6R).<sup>21</sup> On the other hand, however, they do express gp130, a signal transduction element for IL-6, which allows them to respond to IL-6 in the presence of soluble IL-6R (sIL-6R). Indeed, this process of so-called IL-6 trans-signaling plays critical role in controlling chemokine production and contributes to successful resolution of inflammation.<sup>21</sup> The mechanism appears to be particularly active in the acute phase of peritonitis when mesothelial cells release large quantities of IL-6<sup>19</sup> and infiltrating leukocytes shed sufficient levels of sIL-6R.<sup>21</sup> Interestingly, viral IL-6 (vIL-6) that binds directly to gp130 in a process resembling IL-6 trans-signaling, is also capable of inducing VEGF in mesothelial cells.<sup>22</sup>

We have therefore hypothesized that IL-6 together with sIL-6R might be important in controlling VEGF production in human peritoneal mesothelial cells (HPMC). Here, we characterized the transcriptional regulation of VEGF in HPMC and identified transcription factors STAT3 and SP4 as forming a novel axis linking IL-6 and VEGF production in the peritoneum.

## RESULTS

### Induction of VEGF by IL-6 and sIL-6R in mesothelial cells

Since mesothelial cells are the main source of peritoneal VEGF, we have examined whether VEGF production by human peritoneal mesothelial cells (HPMC) can be regulated by IL-6 – either directly through classical IL-6 receptor signaling or IL-6 trans-signaling. Indeed, neither IL-6 nor sIL-6R alone had significant effect on VEGF protein release. However, simultaneous exposure to IL-6+sIL-6R resulted in a significant time- and dose-dependent increase in VEGF secretion (Fig. 1A and 1B). The greatest effect was achieved with both IL-6 and sIL-6R at a dose of 100 ng/ml. This effect was confirmed by specific blocking experiments. Here, antibodies against either IL-6 or sIL-6R, but not with control IgG, inhibited the induction of VEGF by HPMC (Fig. 1C). The effect exerted by a combination of IL-6 and sIL-6R on VEGF secretion was accompanied by a corresponding increase in *VEGF* mRNA (Fig. 1D). These observations prompted us to examine in more detail the signaling events leading to *VEGF* gene induction.

### Activation of VEGF gene promoter by IL-6 and sIL-6R

To investigate how the IL-6+sIL-6R complex impacts on the activity of the *VEGF* gene promoter, HPMC were transiently transfected with *VEGF* luciferase reporter gene constructs and stimulated with IL-6 and sIL-6R. This resulted in a time-dependent increase in VEGF promoter activity, which peaked at 6 hours (Fig. 2A). Exposure for 6 hours to IL-6 or sIL-6R alone had no stimulatory effect on the full length *VEGF* promoter. In contrast, the combination of IL-6 and sIL-6R strongly increased the activity of the *VEGF* promoter (Fig. 2B). To identify *VEGF* promoter regions mediating the response to IL-6 trans-signaling, functional

5'-deletions of the *VEGF* promoter were generated. Truncation of the promoter region spanning positions -268 to -53 resulted in a loss of *VEGF* promoter activity to respond to stimulation with IL-6+sIL-6R (Figure 2C). This result suggested that the region identified comprised essential regulatory elements for the *VEGF* promoter activity. The *in silico* analysis predicted that the region contained high affinity binding sites for the transcription factors SP1 and SP4. To determine which of these transcription factors was regulated by IL-6+sIL-6R, electrophoretic mobility shift assays (EMSA) was performed.

#### **Activation of the transcription factor SP4 by IL-6 and sIL6-R**

EMSA was performed using biotin-labeled double-stranded oligonucleotides corresponding to positions -59 to -82 (SP4) and -80 to -103 (SP1) of the *VEGF* promoter. Analysis of nuclear extracts from cells stimulated with IL-6+sIL-6R showed formation of a prominent DNA-protein complex with a consensus oligonucleotide for SP4 binding (Fig. 3A). No binding was however seen with a consensus motif for SP1. Nuclear extracts from cells stimulated singly with IL-6 and sIL-6R failed to produce any effect.

To verify the specificity of SP4 binding, EMSA was performed with a 100-fold molar excess of an unlabeled SP4 consensus oligonucleotide (Fig. 3B). This competition assay inhibited detection of the SP4-DNA complex. In turn, EMSA with a specific anti-SP4 antibody led to a supershift of the DNA-protein complex (Fig. 3B). Furthermore, transfection of a mutant construct specific to the SP4 binding site completely eliminated *VEGF* promoter activation after IL-6+sIL-6R stimulation (Fig. 3C).

#### **Effect of STAT3 blockade on VEGF production**

As SP4 has not been typically associated with IL-6 signal transduction, we examined the activation of STAT3, a key regulator of IL-6 signaling.<sup>23</sup> Indeed, stimulation of HPMC with IL-6+sIL-6R resulted in a time-dependent induction of *STAT3*, but also of *SP4* mRNA (Fig. 4A and 4B). To determine if there exists a link between STAT3, SP4 and VEGF, the expression of *STAT3* gene was blocked by RNA interference. These experiments showed that *STAT3*-targeting siRNA, but not a scrambled siRNA control, inhibited STAT3 itself at a protein and mRNA level (Fig. 4C and 4D). It also inhibited *SP4* and *VEGF* induction by IL-6+sIL-6R (Fig. 4E and 4F).

#### **Effect of SP4 blockade on VEGF production and angiogenesis**

To further confirm the involvement of SP4 in VEGF production and biological activity, HPMC were stimulated with IL-6+sIL-6R in the presence of either *SP4*-targeting siRNA or scrambled siRNA. The *SP4* blockade resulted in a significant inhibition of VEGF protein release (Fig. 5A). To test the functional properties of the VEGF production, conditioned medium from stimulated HPMC was transferred to endothelial cell cultures and the formation of capillaries assessed. Incubation of human umbilical vein endothelial cells (of the EA.hy926 line) in the presence of conditioned medium from IL-6+sIL-6R-stimulated HPMC significantly increased endothelial cell tube formation. Similar degree of stimulation was observed when conditioned medium from HPMC treated with scrambled siRNA was used. However, endothelial cell angiogenesis was significantly less in response to conditioned medium from HPMC treated with siRNA against *SP4* (Fig. 5B). This effect was not unique to specific features of EA.hy926 endothelial cells, but was also observed in cultures of human dermal microvascular endothelial cells (Supplemental Fig. 1).

### **Effect of IL-6 signaling on peritoneal *Sp4* and *Vegf* expression in mice**

To test whether IL-6 signaling modulates *Vegf* expression during peritoneal inflammation, wild-type (WT) and IL-6-deficient (*IL6*<sup>-/-</sup>) mice were challenged (i.p.) with a cell-free supernatant prepared from a clinical isolate of *Staphylococcus epidermidis* (SES).<sup>21</sup> At designated time points, *Sp4* and *Vegf* expression in the samples of parietal peritoneum was analyzed by qPCR. As illustrated in Fig. 6A, SES-induced inflammation in WT mice was associated with a time-dependent increase in *Vegf* mRNA expression. In contrast, *Vegf* expression was significantly less in *IL6*<sup>-/-</sup> mice. To assess whether this effect was related to sIL-6R activity, WT mice were treated with SES together with soluble gp130 (sgp130), which inhibits IL-6 trans-signaling by the IL-6+sIL-6R complex, but does not inhibit classic IL-6 signaling through IL-6R.<sup>24</sup> Addition of sgp130 significantly decreased *Vegf* expression in WT mice, which resembled the effect seen in *IL6*<sup>-/-</sup> mice and indicated that sIL-6R-mediated effects were involved in regulation of VEGF expression in the inflamed peritoneum.

Having identified SP4 as a mediator of IL-6 trans-signaling in human cells, we next examined peritoneal expression of *Sp4* in mice. Induction of peritoneal inflammation with SES led to a time-dependent increase in *Sp4* expression in WT mice, but not in *IL6*<sup>-/-</sup> animals. In WT mice administered with sgp130, the expression of *Sp4* followed the pattern seen in *IL6*<sup>-/-</sup> mice (Fig. 6B).

### **Effect of IL-6 signaling in mice on peritoneal expression of genes essential for VEGF activity**

To determine whether VEGF induced in the peritoneum by IL-6-signaling can initiate events leading to increased vascular permeability and angiogenesis, we examined expression of several key endothelial-specific targets involved in these processes.<sup>25</sup> These included VEGF receptors (*Vegfr2* and *Vegfr3*), junctional proteins – vascular endothelial cadherin (*VE-Cad*)

and platelet/endothelial cell adhesion molecule 1 (*Pecam1*), markers of arterial commitment – neuropilin 1 (*Nrp1*) and ephrinB2 (*Efnb2*), and a marker of lymphatic commitment – podoplanin (*Pdpn*). Expression of all these angiogenesis-related targets increased significantly within 24 hours of SES-induced inflammation in WT mice but not in *IL6*<sup>-/-</sup> mice and not in WT mice receiving sgp130 (Fig. 7).

#### Effect of IL-6 signaling on peritoneal vasculature during recurrent inflammation in mice

To test whether these acute consequences of increased IL-6 signaling are associated with changes in peritoneal vasculature in the long term, we analyzed the parietal peritoneum of WT and *IL6*<sup>-/-</sup> mice challenged repeatedly with SES, as described previously.<sup>26</sup> After four sequential rounds of acute inflammation, the parietal peritoneum of WT animals appeared only modestly vascularized, but consistently showed increased numbers of vessels staining positively for PECAM-1 (CD31) and podoplanin (gp38) in comparison with *IL6*<sup>-/-</sup> mice (Supplemental Fig.2).

Deleted: see  
Deleted: can be

#### Effect of STAT3/SP4-mediated IL-6 signaling on dialysate-induced VEGF expression in peritonitis

As peritoneal effluents may contain high levels of IL-6 and sIL-6R during peritonitis, we have asked whether such effluents could induce VEGF in HPMC through a signaling pathway identified. Confirming earlier reports,<sup>21;27</sup> we have detected significantly elevated concentrations of IL-6 and sIL-6R in the dialysate drained from PD patients during an acute phase of peritonitis (Fig. 8A). When an exemplary PD effluent from a patient with peritonitis was added to the culture medium, it stimulated *VEGF*, *STAT3* and *SP4* mRNA expression in a concentration-dependent manner (Fig. 8B). The increase in *VEGF* mRNA was reduced to

control levels in the presence of either *STAT3* siRNA or *SP4* siRNA, but not of the scrambled siRNA (Fig. 8C). Interestingly, the inhibition of *STAT3* signaling resulted also in a decreased expression of *SP4* and *STAT3* itself. In contrast, the *SP4* blockade reduced the expression of *SP4*, but not of *STAT3*.

## DISCUSSION

The diversity of IL-6 functions is now well appreciated.<sup>28</sup> These pleiotropic activities are partly related to the complexity of IL-6 signaling, which allows even cells without the cognate IL-6R to respond to IL-6. Here, we demonstrate through a series of *in vitro* and *in vivo* experiments and the analysis of clinical samples from PD patients that a mechanism of IL-6 trans-signaling can contribute significantly to peritoneal VEGF production. In this respect, we have found that the complex of IL-6 and sIL-6R but not IL-6 alone is capable of inducing *de novo* VEGF synthesis in HPMC. In the clinical setting, this is most likely to occur during peritonitis since sIL-6R can be then delivered by shedding from infiltrating neutrophils.<sup>21;29</sup> Indeed, we have observed that peritoneal inflammation induced in mice by *S. epidermidis*,<sup>21</sup> a major causative microorganism of PD-associated peritonitis, resulted in an up-regulation of peritoneal *Vegf* expression. In contrast, the animals deficient in IL-6 failed to produce such a response. A similar lack of effect could be observed in wild-type mice treated with sgp130. These findings indicated that the induction of *Vegf* was controlled through sIL-6R rather than by the membrane-bound IL-6R. This mechanism has previously been demonstrated to be instrumental in coordinating leukocyte trafficking during peritonitis.<sup>21</sup>

Since *STAT3* is the major signal transducer downstream of gp130<sup>23;30</sup> and its involvement in *VEGF* gene regulation has already been postulated,<sup>31-33</sup> we have examined

the consequences of STAT3 inhibition in HPMC. Indeed, the blockade of STAT3 resulted in an inability of the IL-6+sIL-6R complex to induce VEGF. Surprisingly, however, the progressive 5'-deletion analysis mapped the IL-6+sIL-6R response element of the *VEGF* promoter in HPMC to a region that did not contain STAT3 binding elements. Instead, it did contain high affinity binding sites for SP4. Subsequent experiments using EMSA and site-directed mutagenesis confirmed that it was SP4 driving *VEGF* gene expression in response to IL-6 trans-signaling. Moreover, the blockade of STAT3 inhibited *SP4* expression, which positioned STAT3 upstream of SP4 in the signaling cascade. Whilst the targeting of other transcription factors by STAT3 is recognized,<sup>34</sup> the induction of SP4 has not been reported before. The existence of such a signaling axis *in vivo* was further supported by the observation that *S. epidermidis*-induced peritoneal inflammation either in *IL-6*<sup>-/-</sup> mice or in WT mice administered with sgp130 did not produce an increase in peritoneal *Sp4* expression.

The potential of IL-6 to drive *VEGF* expression has been observed in several cancer cells<sup>31;32;35-37</sup> and implicated in tumor-associated angiogenesis.<sup>38;39</sup> Interestingly, it has been demonstrated that anti-IL-6 antibody siltuximab reduced STAT3 activation and angiogenesis in IL-6-producing intraperitoneal ovarian cancer xenografts and reduced VEGF levels in patients with ovarian cancer.<sup>40</sup> The exact role of SP4 in these processes remains to be established. The experiments using RNA interference suggested that SP4 might contribute to the regulation of basal *VEGF* expression in some pancreatic cancer cells lines.<sup>41</sup> The involvement of SP4 could also be inferred from the observation that the down-regulation of *VEGF* expression by cyclooxygenase inhibitors in human colon cancer cells was associated with proteasomal degradation of SP4.<sup>42</sup>

Ablation of STAT3 has long been considered an attractive therapeutic strategy for IL-6-mediated inflammation and cancer.<sup>43;44</sup> Our findings suggest that SP4 activity is

downstream of STAT3 activation in response to IL-6 trans-signaling. Thus, a therapeutic targeting of SP4 may block specific aspects of IL-6 signaling, whilst leaving STAT3 activity intact. That blocking SP4 can indeed produce viable biological effects could be demonstrated by experiments that showed a decrease in angiogenesis induced by conditioned media from HPMC exposed to the IL-6+sIL-6R complex in the presence of *SP4*-silencing RNA.

The consequences of VEGF up-regulation by IL-6 trans-signaling in the setting of PD can be twofold. As VEGF is a potent vascular permeabilizing agent, its rise during acute peritonitis will cause extravasation of fluid rich in plasma proteins, which together with migrating leukocytes will form an inflammatory infiltrate essential for the clearance of infection. The process would be self-limiting given the massive, but short-lived increase in intraperitoneal IL-6 levels<sup>21,27</sup> and the role of IL-6 trans-signaling in suppressing neutrophil-specific chemokines<sup>21</sup> and promoting neutrophil apoptosis.<sup>45</sup> Indeed, it has been demonstrated that the IL-6+sIL-6R complex can induce STAT3- and VEGF-mediated vascular leakage through microvascular endothelial cells.<sup>46</sup>

On the other hand, repeated episodes of peritonitis and the persistent IL-6+sIL-6R-mediated VEGF stimulation may lead to formation of new hyperpermeable blood vessels, as found in many chronic inflammatory diseases.<sup>47</sup> The accumulation of fibrin in tissues favors fibroblast migration and subsequent extracellular matrix synthesis. In this respect, it has recently been demonstrated that recurrent peritoneal inflammation in mice leads to tissue fibrosis through a process that is strictly dependent on IL-6, albeit in this particular model related to STAT1 and IFN- $\gamma$  signaling.<sup>26</sup> Moreover, it has been demonstrated that experimental peritoneal fibrosis in mice could be reduced by antagonizing VEGF through soluble VEGF type I receptor.<sup>48</sup> **We observed that SES-induced inflammation in WT mice was associated with increased expression of key mediators of VEGF signaling, new vessel**

formation<sup>25</sup> and vascular remodeling.<sup>49</sup> In this respect, increased expression of *Pecam1* and *VE-Cad* likely reflect endothelial cell expansion *in vivo* but might also be a secondary response, either to transient rearrangement of intercellular junctions that underlie increased permeability or to degradation of junctional proteins by inflammation-induced proteases.<sup>50</sup> Importantly, these increases in endothelial markers were mediated directly by IL-6 trans-signaling as they did not occur in *IL-6*<sup>-/-</sup> mice and could be reduced in WT mice by specific blockade with sgp130.

Moreover, these early events in IL-6 signaling during acute inflammation may also contribute to chronic changes in the peritoneal vasculature. We have observed increased immunostaining for PECAM-1 and podoplanin in WT mice subjected to repeated episodes of peritonitis compared with *IL-6*<sup>-/-</sup> mice. Of particular interest is the increased number of podoplanin-positive cells in this setting, as increased expression of podoplanin was consistently detected in PD patients with encapsulating peritoneal sclerosis (EPS).<sup>51;52</sup> Furthermore, recent data from the GLOBAL study showed that patients who developed EPS had earlier had higher dialysate levels of IL-6 during PD.<sup>53</sup>

These two scenarios would fit well into the concept that depending on a pathophysiological context, IL-6 can either be crucial for host defense or promote chronic disease.<sup>28</sup> Here, we demonstrate that dialysate IL-6 and sIL-6R can act together through the trans-signaling pathway controlled by the STAT3-SP4 axis to up-regulate mesothelial VEGF production during peritonitis. The identification of this novel mechanism that controls peritoneal *VEGF* expression at the transcriptional level may help to understand better how peritoneal inflammation and angiogenesis contribute to adverse peritoneal membrane remodeling during peritoneal dialysis.

Deleted: an

## **CONCISE METHODS**

### **Materials**

Unless stated otherwise, all chemicals were from Sigma-Aldrich (St Louis, MO, USA) and all culture plastics were Falcon® from Becton Dickinson (Franklin Lakes, NJ, USA). Cell culture media and buffers were from Biochrom AG (Berlin, Germany) and fetal calf serum was from Invitrogen (Darmstadt, Germany). Human recombinant IL-6 and sIL-6R were from R&D Systems (Wiesbaden, Germany). Antibodies against STAT3 and SP4 were from Santa Cruz Biotechnology, Inc. (Heidelberg, Germany).

### **Mesothelial cell culture**

HPMC were isolated from the specimens of omentum obtained from consenting patients undergoing elective abdominal surgery. Cells were cultured and characterized as described in detail elsewhere.<sup>20</sup> For the experiments, cells were rendered quiescent by serum deprivation for 48 hours and then stimulated with IL-6 and/or sIL-6R as specified in the legends to figures. All experiments were performed with cells no older than from the third passage to minimize the number of senescent cells, as this may affect the level of VEGF released.<sup>54</sup>

### **Endothelial cell culture and tube formation assay**

Human umbilical vein endothelial cells (HUVEC) of the EA.hy926 line<sup>55</sup> were kindly donated by Dr. CJ Edgell (University of North Carolina, Chapel Hill, USA). For the tube formation assay, Matrigel (Corning, Tewksbury, MA, USA) was poured onto a 96-well plate (50 µl/well) and solidified at 37°C for 30 min. Endothelial cells ( $2 \times 10^4$  cells/well) were

seeded onto the Matrigel and cultured in MCDB131 medium (Thermo Fisher Scientific, Waltham, MA USA) with or without 10% (v/v) conditioned medium from HPMC treated with as described in the legends to figures. Capillary networks of tubes formed were photographed under the microscope (Zeiss Axiovert 40 CFL Oberkochen, Germany) and five randomly selected fields from each well were analyzed for total capillary length using ImageJ 1.43 software.<sup>56</sup>

### **Immunoassays**

Concentrations of VEGF, IL-6 and sIL-6R were measured using DuoSet<sup>®</sup> Immunoassay Kits (R&D Systems). All assays were designed and performed as per manufacturer's instructions.

### **Gene expression analysis**

The expression of target genes was assessed with reverse transcription and quantitative PCR (RT-qPCR), essentially as described previously.<sup>20</sup> PCR conditions and primer sequences were as specified in Supplemental Data.

### **DNA Constructs and Reporter Plasmids**

Progressive VEGF 5'-deletion luciferase plasmids (pLuc 2068, pLuc 1340, pLuc 840, pLuc 318, and pLuc 102) were kindly provided by Dr. A. Scholz (Charité-Universitätsmedizin, Berlin, Germany). The constructs were generated as reported previously,<sup>57</sup> and checked for the correct length by restriction digest. To target the SP4 binding site at position -73 to 75 (TGA) within the *VEGF* promoter, the desired sequence (AAA) was inserted into the pLuc VEGF 318 construct using the Q5 site-directed mutagenesis kit (New England BioLabs,

Franfurt, Germany) with forward primer 5'- GGGGCGGGCCaaaGGCGGGGTCCC -3' and reverse primer 5'- GGGGGCGGGGACAGGCG -3'.

### **Transfection studies**

Transient transfection and luciferase assays were performed as previously described in detail.<sup>20</sup> Transfections with siRNAs were performed with the siRNA Transfection Reagent and siRNAs for *STAT3* (sc-44275), *SP4* (sc-36545), or with scrambled siRNA control (sc-37007) as per manufacturer's instructions (all materials from Santa Cruz Biotechnology, Heidelberg, Germany).

### **Computational analysis of the VEGF promoter**

The human *VEGF* promoter region -268 to -51 (GenBank NT\_007592.15) was analyzed by PROMO virtual laboratory ([http://algggen.lsi.upc.es/cgi-bin/promo\\_v3/promo/promoinit.cgi?dirDB=TF\\_8.3](http://algggen.lsi.upc.es/cgi-bin/promo_v3/promo/promoinit.cgi?dirDB=TF_8.3)) for the presence and location of potential transcription factor binding sites.

### **Nuclear extracts and electrophoretic mobility shift assay**

Nuclear extracts were prepared using the NE-PER Nuclear and Cytoplasmic Extraction Kit (Thermo Scientific, Darmstadt, Germany) according to the manufacturer's instructions. The extracts obtained were aliquoted and stored at -80°C. Oligonucleotide probes were labeled with the Biotin 3' End DNA Labeling Kit (Thermo Scientific). For the electrophoretic mobility shift assay (EMSA) the following probes were used (the corresponding region of the *VEGF* promoter is given in brackets): *SP4* - 5'- GCGGGCCGGGGCGGGTCCCGGC -3' (-131 to -154), *Sp1* - 5'- TCGCCTGTCCCCGCCCCCGGGGC -3' (-109 to -132). Each binding mixture (20 µl) for

EMSA contained 5 µg nuclear extract, 20 fmol labeled double-stranded probe, 1 µg poly-dI/dC, and 2 µl 10 x reaction buffer and was incubated at room temperature for 30 min. The protein-DNA complexes were then analyzed by electrophoresis in 6% non-denaturing polyacrylamide gels and visualized using a LightShift Chemiluminescent EMSA Kit (Thermo Scientific).

### **Western blotting**

Cell extracts were prepared as described,<sup>58</sup> electrophoresed on sodium dodecyl sulfate-polyacrylamide gels and Western blotted using antibodies against STAT3 and SP4 (Santa Cruz Biotechnology), GAPDH (Hyttest, Turku, Finland), and appropriate secondary peroxidase-conjugated IgG (Dianova, Hamburg, Germany). The bands obtained were visualized and analyzed using Enhanced Chemiluminescence Detection System (Thermo Scientific) and Image J 1.43 software (National Institutes of Health, USA).

### **Peritoneal dialysis effluent**

Peritoneal effluent was obtained from consenting patients undergoing continuous ambulatory PD. Dialysate was collected either from stable PD patients after a routine 4-hr dwell or from the first bag drained from patients presenting with an episode of peritonitis. Samples were processed as described previously.<sup>59</sup>

### **Animal experiments**

All animal procedures were performed under appropriate licenses and according to institutional animal care guidelines. The experiments were performed in weight-matched 7- to 12-wk-old inbred C57BL/6J wild-type (WT) and IL-6-deficient (*IL6*<sup>-/-</sup>) mice, as previously

described.<sup>45</sup> Peritoneal inflammation was established through i.p. administration of 500 µl of a cell-free supernatant (SES) prepared from *S. epidermidis* isolated from a PD patient, as detailed elsewhere.<sup>60</sup> Repeated challenge with SES was used to model recurrent peritoneal inflammation, essentially as described previously.<sup>26</sup> Animals were sacrificed at designated time points and specimens of peritoneal peritoneum were collected and snap frozen in liquid nitrogen. The tissue samples were then homogenized in Tri Reagent (Invitrogen) and total RNA was prepared according to the manufacturer's instructions. Additional biopsy samples were processed for immunohistochemistry, as described<sup>26</sup> and subsequently stained with antibodies against anti-CD31 (eBioscience) and podoplanin (BioLegend). Antibody labeling was detected using biotinylated secondary antibodies (Dako), the Vectastain ABC kit and diaminobenzidine chromagen (Vector Laboratories). Sections were counterstained with hematoxylin. Quantification of antibody staining was performed using the Leica QWin microscope imaging software (Jones, GW. et al., 2015 J. Exp. Med. 212:1793).

## Statistics

Statistical analysis was performed using GraphPad Prism 6.05 software (GraphPad Software). The data were analyzed with the t-test or repeated measures analysis of variance for paired data (*in vitro* experiments) or unpaired data (animal experiments), as appropriate. Results were expressed as means ± SEM. Differences with a P value <0.05 were considered significant.

Deleted: xxx

Deleted: Staining was visualized with yyy and analyzed with zzz..... ¶

Formatted: Font: +Body (Calibri)

Formatted: Font: +Body (Calibri), 12 pt

Formatted: Font: +Body (Calibri), 12 pt

Formatted: Font: +Body (Calibri), 12 pt

Formatted: Font: 8 pt

Formatted: Normal, Indent: First line: 0 cm, No widow/orphan control, Don't adjust space between Latin and Asian text, Don't adjust space between Asian text and numbers

## **ACKNOWLEDGEMENT**

JW, AR, NT, and AJ were supported by the European Training & Research in Peritoneal Dialysis (EuTRiPD) programme, a project funded by the European Union within the Marie Curie scheme (No. 287813). [RC was supported by Berlin Institute of Health \(BIH\). SAJ has grant funding from Arthritis Research UK and Kidney Research UK. JUF is recipient of a la Caixa PhD Studentship awarded through the British Council.](#)

## **DISCLOSURES**

The authors declare that there is no conflict of interest to disclose.

## REFERENCES

1. Davies SJ, Mushahar L, Yu Z, Lambie M: Determinants of peritoneal membrane function over time. *Semin Nephrol* 31:172-182, 2011
2. Heimbürger O, Waniewski J, Werynski A, Tranaeus A, Lindholm B: Peritoneal transport in CAPD patients with permanent loss of ultrafiltration capacity. *Kidney Int* 38:495-506, 1990
3. Ho-Dac-Pannekeet MM, Atasever B, Struijk DG, Krediet RT: Analysis of ultrafiltration failure in peritoneal dialysis patients by means of standard peritoneal permeability analysis. *Perit Dial Int* 17:144-150, 1997
4. Williams JD, Craig KJ, Topley N, Von Ruhland C, Fallon M, Newman GR, Mackenzie RK, Williams GT: Morphologic changes in the peritoneal membrane of patients with renal disease. *J Am Soc Nephrol* 13:470-479, 2002
5. Williams JD, Craig KJ, Von Ruhland C, Topley N, Williams GT: The natural course of peritoneal membrane biology during peritoneal dialysis. *Kidney Int Suppl* 43-49, 2003
6. Mateijsen MA, van der Wal AC, Hendriks PM, Zweers MM, Mulder J, Struijk DG, Krediet RT: Vascular and interstitial changes in the peritoneum of CAPD patients with peritoneal sclerosis. *Perit Dial Int* 19:517-525, 1999
7. Margetts PJ, Gyorffy S, Kolb M, Yu L, Hoff CM, Holmes CJ, Gaudie J: Antiangiogenic and antifibrotic gene therapy in a chronic infusion model of peritoneal dialysis in rats. *J Am Soc Nephrol* 13:721-728, 2002
8. Nagy JA, Dvorak AM, Dvorak HF: VEGF-A and the induction of pathological angiogenesis. *Annu Rev Pathol* 2:251-275, 2007
9. Szeto CC, Chow KM, Poon P, Szeto CY, Wong TY, Li PK: Genetic polymorphism of VEGF: Impact on longitudinal change of peritoneal transport and survival of peritoneal dialysis patients. *Kidney Int* 65:1947-1955, 2004
10. Pecoits-Filho R, Araujo MR, Lindholm B, Stenvinkel P, Abensur H, Romao JE, Jr., Marcondes M, De Oliveira AH, Noronha IL: Plasma and dialysate IL-6 and VEGF concentrations are associated with high peritoneal solute transport rate. *Nephrol Dial Transplant* 17:1480-1486, 2002
11. Rodrigues AS, Martins M, Korevaar JC, Silva S, Oliveira JC, Cabrita A, Castro e Melo, Krediet RT: Evaluation of peritoneal transport and membrane status in peritoneal dialysis: focus on incident fast transporters. *Am J Nephrol* 27:84-91, 2007
12. Witowski J, Jörres A: Angiogenic activity of the peritoneal mesothelium: implications for peritoneal dialysis. In: *Progress in peritoneal dialysis*, edited by Krediet RT, Rijeka, In-Tech, 2011, pp 61-74

13. Pecoits-Filho R, Carvalho MJ, Stenvinkel P, Lindholm B, Heimbürger O: Systemic and intraperitoneal interleukin-6 system during the first year of peritoneal dialysis. *Perit Dial Int* 26:53-63, 2006
14. Oh KH, Jung JY, Yoon MO, Song A, Lee H, Ro H, Hwang YH, Kim DK, Margetts P, Ahn C: Intra-peritoneal interleukin-6 system is a potent determinant of the baseline peritoneal solute transport in incident peritoneal dialysis patients. *Nephrol Dial Transplant* 25:1639-1646, 2010
15. Lambie M, Chess J, Donovan KL, Kim YL, Do JY, Lee HB, Noh H, Williams PF, Williams AJ, Davison S, Dorval M, Summers A, Williams JD, Bankart J, Davies SJ, Topley N: Independent effects of systemic and peritoneal inflammation on peritoneal dialysis survival. *J Am Soc Nephrol* 24:2071-2080, 2013
16. Aroeira LS, Aguilera A, Selgas R, Ramirez-Huesca M, Perez-Lozano ML, Cirugeda A, Bajo MA, del Peso G, Sanchez-Tomero JA, Jimenez-Heffernan JA, Lopez-Cabrera M: Mesenchymal conversion of mesothelial cells as a mechanism responsible for high solute transport rate in peritoneal dialysis: role of vascular endothelial growth factor. *Am J Kidney Dis* 46:938-948, 2005
17. Gerber SA, Rybalko VY, Bigelow CE, Lugade AA, Foster TH, Frelinger JG, Lord EM: Preferential attachment of peritoneal tumor metastases to omental immune aggregates and possible role of a unique vascular microenvironment in metastatic survival and growth. *Am J Pathol* 169:1739-1752, 2006
18. Topley N, Jörres A, Luttmann W, Petersen MM, Lang MJ, Thierauch KH, Müller C, Coles GA, Davies M, Williams JD: Human peritoneal mesothelial cells synthesize interleukin-6: induction by IL-1 beta and TNF alpha. *Kidney Int* 43:226-233, 1993
19. Witowski J, Jörres A, Coles GA, Williams JD, Topley N: Superinduction of IL-6 synthesis in human peritoneal mesothelial cells is related to the induction and stabilization of IL-6 mRNA. *Kidney Int* 50:1212-1223, 1996
20. Catar R, Witowski J, Wagner P, Annett S, I, Kawka E, Philippe A, Dragun D, Jorres A: The proto-oncogene c-Fos transcriptionally regulates VEGF production during peritoneal inflammation. *Kidney Int* 84:1119-1128, 2013
21. Hurst SM, Wilkinson TS, McLoughlin RM, Jones S, Horiuchi S, Yamamoto N, Rose-John S, Fuller GM, Topley N, Jones SA: IL-6 and its soluble receptor orchestrate a temporal switch in the pattern of leukocyte recruitment seen during acute inflammation. *Immunity* 14:705-714, 2001
22. Fielding CA, McLoughlin RM, Colmont CS, Kovaleva M, Harris DA, Rose-John S, Topley N, Jones SA: Viral IL-6 blocks neutrophil infiltration during acute inflammation. *J Immunol* 175:4024-4029, 2005
23. Heinrich PC, Behrmann I, Haan S, Hermanns HM, Müller-Newen G, Schaper F: Principles of interleukin (IL)-6-type cytokine signalling and its regulation. *Biochem J* 374:1-20, 2003

24. Jostock T, Mullberg J, Ozbek S, Atreya R, Blinn G, Voltz N, Fischer M, Neurath MF, Rose-John S: Soluble gp130 is the natural inhibitor of soluble interleukin-6 receptor transsignaling responses. *Eur J Biochem* 268:160-167, 2001
25. Udan RS, Culver JC, Dickinson ME: **Understanding vascular development.** *Wiley Interdiscip Rev Dev Biol* 2:327-346, 2013
26. Fielding CA, Jones GW, McLoughlin RM, McLeod L, Hammond VJ, Uceda J, Williams AS, Lambie M, Foster TL, Liao CT, Rice CM, Greenhill CJ, Colmont CS, Hams E, Coles B, Kift-Morgan A, Newton Z, Craig KJ, Williams JD, Williams GT, Davies SJ, Humphreys IR, O'Donnell VB, Taylor PR, Jenkins BJ, Topley N, Jones SA: Interleukin-6 signaling drives fibrosis in unresolved inflammation. *Immunity* 40:40-50, 2014
27. Goldman M, Vandenabeele P, Moulart J, Amraoui Z, Abramowicz D, Nortier J, Vanherweghem JL, Fiers W: Intraperitoneal secretion of interleukin-6 during continuous ambulatory peritoneal dialysis. *Nephron* 56:277-280, 1990
28. Hunter CA, Jones SA: IL-6 as a keystone cytokine in health and disease. *Nat Immunol* 16:448-457, 2015
29. Chalaris A, Rabe B, Paliga K, Lange H, Laskay T, Fielding CA, Jones SA, Rose-John S, Scheller J: Apoptosis is a natural stimulus of IL6R shedding and contributes to the proinflammatory trans-signaling function of neutrophils. *Blood* 110:1748-1755, 2007
30. Ernst M, Thiem S, Nguyen PM, Eissmann M, Putoczki TL: Epithelial gp130/Stat3 functions: an intestinal signaling node in health and disease. *Semin Immunol* 26:29-37, 2014
31. Wei D, Le X, Zheng L, Wang L, Frey JA, Gao AC, Peng Z, Huang S, Xiong HQ, Abbruzzese JL, Xie K: Stat3 activation regulates the expression of vascular endothelial growth factor and human pancreatic cancer angiogenesis and metastasis. *Oncogene* 22:319-329, 2003
32. Loeffler S, Fayard B, Weis J, Weissenberger J: Interleukin-6 induces transcriptional activation of vascular endothelial growth factor (VEGF) in astrocytes in vivo and regulates VEGF promoter activity in glioblastoma cells via direct interaction between STAT3 and Sp1. *Int J Cancer* 115:202-213, 2005
33. Jenkins BJ, Grail D, Nheu T, Najdovska M, Wang B, Waring P, Inglese M, McLoughlin RM, Jones SA, Topley N, Baumann H, Judd LM, Giraud AS, Boussioutas A, Zhu HJ, Ernst M: Hyperactivation of Stat3 in gp130 mutant mice promotes gastric hyperproliferation and desensitizes TGF-beta signaling. *Nat Med* 11:845-852, 2005
34. Carpenter RL, Lo HW: STAT3 Target Genes Relevant to Human Cancers. *Cancers (Basel)* 6:897-925, 2014
35. Su JL, Lai KP, Chen CA, Yang CY, Chen PS, Chang CC, Chou CH, Hu CL, Kuo ML, Hsieh CY, Wei LH: A novel peptide specifically binding to interleukin-6 receptor (gp80) inhibits angiogenesis and tumor growth. *Cancer Res* 65:4827-4835, 2005

36. Adachi Y, Aoki C, Yoshio-Hoshino N, Takayama K, Curiel DT, Nishimoto N: Interleukin-6 induces both cell growth and VEGF production in malignant mesotheliomas. *Int J Cancer* 119:1303-1311, 2006
37. Huang SP, Wu MS, Shun CT, Wang HP, Lin MT, Kuo ML, Lin JT: Interleukin-6 increases vascular endothelial growth factor and angiogenesis in gastric carcinoma. *J Biomed Sci* 11:517-527, 2004
38. Yao X, Huang J, Zhong H, Shen N, Faggioni R, Fung M, Yao Y: Targeting interleukin-6 in inflammatory autoimmune diseases and cancers. *Pharmacol Ther* 141:125-139, 2014
39. Middleton K, Jones J, Lwin Z, Coward JI: Interleukin-6: an angiogenic target in solid tumours. *Crit Rev Oncol Hematol* 89:129-139, 2014
40. Coward J, Kulbe H, Chakravarty P, Leader D, Vassileva V, Leinster DA, Thompson R, Schioppa T, Nemeth J, Vermeulen J, Singh N, Avril N, Cummings J, Rexhepaj E, Jirstrom K, Gallagher WM, Brennan DJ, McNeish IA, Balkwill FR: Interleukin-6 as a therapeutic target in human ovarian cancer. *Clin Cancer Res* 17:6083-6096, 2011
41. Abdelrahim M, Smith R, III, Burghardt R, Safe S: Role of Sp proteins in regulation of vascular endothelial growth factor expression and proliferation of pancreatic cancer cells. *Cancer Res* 64:6740-6749, 2004
42. Abdelrahim M, Safe S: Cyclooxygenase-2 inhibitors decrease vascular endothelial growth factor expression in colon cancer cells by enhanced degradation of Sp1 and Sp4 proteins. *Mol Pharmacol* 68:317-329, 2005
43. O'shea JJ, Holland SM, Staudt LM: JAKs and STATs in immunity, immunodeficiency, and cancer. *N Engl J Med* 368:161-170, 2013
44. Taniguchi K, Karin M: IL-6 and related cytokines as the critical lynchpins between inflammation and cancer. *Semin Immunol* 26:54-74, 2014
45. McLoughlin RM, Witowski J, Robson RL, Wilkinson TS, Hurst SM, Williams AS, Williams JD, Rose-John S, Jones SA, Topley N: Interplay between IFN-gamma and IL-6 signaling governs neutrophil trafficking and apoptosis during acute inflammation. *J Clin Invest* 112:598-607, 2003
46. Wei LH, Chou CH, Chen MW, Rose-John S, Kuo ML, Chen SU, Yang YS: The role of IL-6 trans-signaling in vascular leakage: implications for ovarian hyperstimulation syndrome in a murine model. *J Clin Endocrinol Metab* 98:E472-E484, 2013
47. Nagy JA, Dvorak AM, Dvorak HF: Vascular hyperpermeability, angiogenesis, and stroma generation. *Cold Spring Harb Perspect Med* 2:a006544, 2012
48. Motomura Y, Kanbayashi H, Khan WI, Deng Y, Blennerhassett PA, Margetts PJ, Gauldie J, Egashira K, Collins SM: The gene transfer of soluble VEGF type I receptor (Flt-1) attenuates peritoneal fibrosis formation in mice but not soluble TGF-beta type II receptor gene transfer. *Am J Physiol Gastrointest Liver Physiol* 288:G143-G150, 2005

49. Baeyens N, Bandyopadhyay C, Coon BG, Yun S, Schwartz MA: Endothelial fluid shear stress sensing in vascular health and disease. *J Clin Invest* 126:821-828, 2016
50. Wallez Y, Huber P: Endothelial adherens and tight junctions in vascular homeostasis, inflammation and angiogenesis. *Biochim Biophys Acta* 1778:794-809, 2008
51. Yaginuma T, Yamamoto I, Yamamoto H, Mitome J, Tanno Y, Yokoyama K, Hayashi T, Kobayashi T, Watanabe M, Yamaguchi Y, Hosoya T: Increased lymphatic vessels in patients with encapsulating peritoneal sclerosis. *Perit Dial Int* 32:617-627, 2012
52. Braun N, Alscher DM, Fritz P, Edenhofer I, Kimmel M, Gaspert A, Reimold F, Bode-Lesniewska B, Ziegler U, Biegger D, Wuthrich RP, Segerer S: Podoplanin-positive cells are a hallmark of encapsulating peritoneal sclerosis. *Nephrol Dial Transplant* 26:1033-1041, 2011
53. Lambie MR, Chess J, Summers AM, Williams PF, Topley N, Davies SJ: Peritoneal inflammation precedes encapsulating peritoneal sclerosis: results from the GLOBAL Fluid Study. *Nephrol Dial Transplant* 31:480-486, 2016
54. Ksiazek K, Jörres A, Witowski J: Senescence induces a proangiogenic switch in human peritoneal mesothelial cells. *Rejuvenation Res* 11:681-683, 2008
55. Edgell CJ, McDonald CC, Graham JB: Permanent cell line expressing human factor VIII-related antigen established by hybridization. *Proc Natl Acad Sci U S A* 80:3734-3737, 1983
56. Di Marco GS, König M, Stock C, Wiesinger A, Hillebrand U, Reiermann S, Reuter S, Amler S, Köhler G, Buck F, Fobker M, Kumpers P, Oberleithner H, Hausberg M, Lang D, Pavenstadt H, Brand M: High phosphate directly affects endothelial function by downregulating annexin II. *Kidney Int* 83:213-222, 2013
57. Finkenzeller G, Sparacio A, Technau A, Marme D, Siemeister G: Sp1 recognition sites in the proximal promoter of the human vascular endothelial growth factor gene are essential for platelet-derived growth factor-induced gene expression. *Oncogene* 15:669-676, 1997
58. Hegner B, Weber M, Dragun D, Schulze-Lohoff E: Differential regulation of smooth muscle markers in human bone marrow-derived mesenchymal stem cells. *J Hypertens* 23:1191-1202, 2005
59. Witowski J, Tayama H, Ksiazek K, Wanic-Kossowska M, Bender TO, Jörres A: Human peritoneal fibroblasts are a potent source of neutrophil-targeting cytokines: a key role of IL-1 $\beta$  stimulation. *Lab Invest* 2009
60. Mackenzie RK, Topley N, Neubauer A, Coles GA, Williams JD: Staphylococcal exoproducts down-regulate cyclooxygenase 1 and 2 in peritoneal macrophages. *J Lab Clin Med* 129:23-34, 1997

## Figure legends

**Figure 1. Induction of VEGF in HPMC by a combination of IL-6 and sIL-6R.** (A): Kinetics of VEGF secretion by HPMC treated with IL-6 (10 ng/ml) and sIL-6R (25 ng/ml) either singly or in combination; \*P<0.05 vs. control cells at each time point, n=6; (B): Dose effect of IL-6 and sIL-6R on VEGF release over the period of 48 hours; \*P<0.05 vs. untreated cells; (C): Blockade of the effect of the IL-6+sIL-6R complex. HPMC were treated with IL-6+sIL-6R (both at 100 ng/ml) for 48 hours in the presence of 10 µg/ml of antibodies against either IL-6 (MAB206, R&D Systems) or sIL-6R (MAB227, R&D Systems). An additional group received an irrelevant antibody of the same class and at the same dose; \*P<0.05 vs. cells not exposed to antibodies, #P<0.05 vs. cells treated with an irrelevant antibody; n=5; (D): Induction of *VEGF* mRNA by IL-6 and/or sIL-6R. HPMC were treated with IL-6 and sIL-6R (both at 100 ng/ml) either singly or in combination for 48 hours, \*P<0.05 vs. untreated cells n=4).

**Figure 2. Identification of sequences in the human *VEGF* promoter responsive to stimulation with the IL-6+sIL-6R complex.** Cells were transiently transfected with *VEGF* promoter constructs and stimulated with IL-6 and/or sIL-6R (both at 100 ng/ml), as indicated. Luciferase activity was determined as described in Methods. (A): Time effect of the IL-6+sIL-6R complex on the full-length *VEGF* promoter activity \*P<0.05 vs. unstimulated control, n=3; (B): Full-length *VEGF* promoter activity after 6 hours of stimulation with IL-6 and/or sIL-6R, n=4; (C): Effect of progressive 5'-deletions of the *VEGF* promoter on its activity upon stimulation with IL-6+sIL-6R for 6 hours; \*P<0.05 vs. unstimulated controls, n=4.

**Figure 3. Identification of SP4 as a transcription factor mediating human VEGF promoter induction by the IL-6+sIL-6R complex. (A-B):** Cells were stimulated with IL-6+sIL-6R at 100 ng/ml for 6 hours, the nuclear fractions were obtained and analyzed with EMSA. In A, EMSA was performed with consensus oligonucleotide probes for SP1 and SP4; In B, formation of nuclear complexes with SP4 probe was assessed either in the presence of 100-fold molar excess of unlabeled VEGF DNA (resulting in a reduced shift – a lower arrow) or in the presence of SP4-specific antibody (resulting in supershift – an upper arrow). **(C):** Effect of site-directed mutagenesis in the SP4 binding site within the VEGF promoter on its activity after stimulation with IL-6+sIL-6R. #P<0.05 vs. relevant control, n=4.

**Figure 4. The role of STAT3 in SP4-mediated VEGF induction by the IL-6+sIL-6R complex. (A-B):** Kinetics of STAT3 and SP4 mRNA induction in HPMC treated with IL-6+sIL-6R (both at 100 ng/ml); \*P<0.05 vs. control cells at each time point, n=4; **(C-F):** Effect of STAT3 silencing on STAT3, SP4 and VEGF expression. Cells were transiently transfected with either STAT3 siRNA or scrambled (Scramb) siRNA and then stimulated with IL-6+sIL-6R (both at 100 ng/ml) for 9 hours. Cells were assessed for STAT3 protein expression by Western blotting (C) and mRNA expression by qPCR for STAT3 (D), SP4 (E), and VEGF (F). In C, a representative immunoblot is presented together with quantified data from 4 independent experiments. In C-F \*P<0.05 vs. cells stimulated with IL-6+sIL-6R in the absence of siRNA, n=4.

**Figure 5. Effect of SP4 on VEGF-mediated endothelial cell tube formation. (A):** Cells were transiently transfected with either SP4 siRNA or scrambled (Scramb) siRNA, stimulated with IL-6+sIL-6R (both at 100 ng/ml) for 24 hours and then assessed for VEGF secretion, n=5. **(B):** Effect of conditioned medium (10% v/v) from HPMC treated as in (A) on

endothelial cell tube formation within 16 hours. \*P<0.05 vs. cells stimulated with IL-6+sIL-6R in the absence of siRNA, n=4. Representative phase contrast images (magnification 100 X) are presented in order corresponding to experimental groups as shown in graph from left to right.

**Figure 6. Effect of IL-6 signaling on peritoneal *Sp4* and *Vegf* expression in mice.** WT and *IL6*<sup>-/-</sup> mice were intra-peritoneally administered with SES and then analyzed at defined time points for *Sp4* (A) and *Vegf* (B) expression in the parietal peritoneum. An additional group of WT animals received SES together with sgp130 (150 ng/mouse); \*P<0.05 vs. WT mice at the same time point, n=4 mice per condition.

**Figure 7. Effect of IL-6 signaling on peritoneal expression of endothelial-specific targets** Mice were treated as in Fig. 6 and analyzed for peritoneal expression of *Vegfr2* (A), *Vegfr3* (B), *Pecam1* (C), *VE-Cad* (D), *Nrp1* (E), *Efnb2* (F), and *Pdpn* (G). \*P<0.05 vs. WT mice at the same time point, n=4 mice per condition.

**Figure 8. IL-6 signaling contributes to VEGF release by HPMC during peritonitis.** (A): IL-6 and sIL-6R levels in dialysates drained either from stable PD patients after a routine 4-hr dwell (n=20) or from patients with peritonitis at first presentation (n=11); the data are presented as box and whiskers plots, with the median, 25th and 75th percentiles, and range of data indicated; \*P<0.05 between the groups; (B): The dose effect of exemplary PD effluent drained during peritonitis on *VEGF* (top), *STAT3* (middle) and *SP4* (bottom) mRNA expression in HPMC. Cells were treated with increasing doses of effluent for 24 hours. \*P<0.05 vs. untreated controls, n=4; (C): Cells were transiently transfected with 10  $\mu$ M

*STAT3* siRNA, *SP4* siRNA, or scrambled siRNA, as indicated. After that cells were exposed to peritoneal effluent (25% v/v) from a PD patient with peritonitis for 24 hours and assessed for mRNA expression of *VEGF* (top), *STAT3* (middle), and *SP4* (bottom). \*P<0.05 vs. cells treated with the dialysate in the absence of siRNAs, n=4.

## SUPPLEMENTAL DATA

### Gene expression analysis

The expression of target genes was assessed with reverse transcription and quantitative PCR (RT-qPCR). Total RNA was extracted with the PerfectPure RNA Cultured Cell Kit (5 Prime, Hamburg, Germany), reverse transcribed into cDNA with random hexamer primers, and amplified with real-time qPCR on the Applied Biosystems 7500 Fast Real-Time PCR system (Applied Biosystems, Darmstadt, Germany). The reaction was carried out in 14 µl reaction volumes containing 2 µl of cDNA (20 ng), specific sense and anti-sense primers (250 nM each), and 7 µl Power SYBR Green PCR Master Mix (Applied Biosystems). PCR primers were synthesized by TIB Molbiol (Berlin, Germany) and their sequences were as follows:

- *VEGF* (GenBank NM\_001171623.1):  
forward (5'-AAGGAGGAGGGCAGAATCAT-3'),  
reverse (5'-ATCTGCATGGTGATGTTGGA-3');
- *STAT3* (GenBank NM\_139276.2):  
forward 5'- GGCCATCTTGAGCACTAAGC-3'),  
reverse (5'-CGGACTGGATCTGGGTCTTA -3');
- *SP4* (GenBank NM\_003112.3):  
forward 5'-TCAGCAGCAAGGACAAGATG -3'),  
reverse (5'- AAGCCTCTTGCCAGGTTGTA -3');
- *β2M* (GenBank NM\_004048.2):  
forward (5'- GTGCTCGCGCTACTCTCTCT-3'),  
reverse (5'- CGGCAGGCATACTCATCTTT -3').

Primers for murine targets were as follows:

- *Sp4* (GenBank NM\_009239.4):  
forward (5'- GCCTGCTCCTGCCTAACTG -3'),  
reverse (5'- CTCGGAGGTGAGAGGTCTTG -3');
- *Vegf* (GenBank NM\_001025250.3):  
forward (5'- CAGGCTGCTGTAAACGATGAA -3'),  
reverse (5'- GCATTCACATCTGCTGTGCT -3').
- *β2m* (GenBank NM\_009735.3):  
forward (5'- GAAATCCAAATGCTGAAGAACG-3'),  
reverse (5'- CAAATGAATGTTTCAGAGCATCATG -3')
- *Pecam1* (GenBank NM\_008816.2):  
forward (5'- AGAGACGGTCTTGTCGCAGT -3'),  
reverse (5'- TACTGGGCTTCGAGAGCATT -3');
- *VE-Cad* (GenBank NM\_009868.4):  
forward (5'- ACCGAGAGAAACAGGCTGAA -3'),  
reverse (5'- AGACGGGGAAGTTGTCATTG -3');
- *Vegfr2* (GenBank NM\_010612.2):  
forward (5'- GGCGGTGGTGACAGTATCTT -3'),  
reverse (5'- GTCACTGACAGAGGCGATGA -3');
- *Vegfr3* (GenBank NM\_008029.3):  
forward (5'- GCTGTTGGTTGGAGAGAAGC -3'),  
reverse (5'- GAGCCACTCGACTGATGA -3');

- *Efnb2* (GenBank NM\_010111.5):  
forward (5'- CTCAACTGTGCCAGACCAGA -3'),  
reverse (5'- CTTGTTGGACCGTGATTCCT -3');
- *Nrp1* (GenBank NM\_008737.2):  
forward (5'- GGAGCTACTGGGCTGTGAAG -3'),  
reverse (5'- ACCGTATGTCGGGAACTCTG -3');
- *Pdpr* (GenBank **XX**):  
forward (5'- **XX** -3'),  
reverse (5'- **XX** -3');
- 

After an initial activation step for 2 min at 50°C and denaturation at 95°C for 10 min, 40 cycles of 15 sec at 95°C, and 1 min at 60°C were performed. Specificity of the reaction was verified by melting curve analysis at the end of each series of assays. The relative amount of gene transcript was calculated by the cycle threshold method using the Applied Biosystems 7500 System v.1.2.3 software and normalized for the endogenous reference ( $\beta$ -microglobulin).

#### **VEGF promoter, EMSA oligonucleotide sequences and site-directed mutagenesis primer**

-267  
GGGCGGTGTCTCTGGACAGAGTTTCCGGGGCGGATGGGTAATTTTCAGGCTGTGAACCTTGGTG  
GGGGTCGAGCTTCCCCCTTATTGCGGCGGGCTGCGGGCCAGGCTTCACTGAGCGTCCGAGAGCCC  
GGGCCGAGCCGCGTGTGGAAGGCTGAGGCT**TCGCCTGTCCCCGCCCCCGGGGCGGGCCGGGGG**  
**CGGGGTCCCGGC**GGGGCGGAGCCATGCGCCCCCCTTTTTTTTTTAAAAGTCGGCTGGTAGCGGGG  
AGGatcgcggaggcttggggcagccggtagctcggaggtcgtggcctgggg+50

EMSA oligo sequences for SP1 and SP4  
**GCGGGCCGGGGCGGGTCCCGGC** SP4 -59 to -82  
**TCGCCTGTCCCCGCCCCCGGGGC** SP1 -80 to -103

Site directed mutagenesis of SP4 sequences

**GGGGCGGGCC**aaaGGCGGGTCCC site directed mutagenesis forward Primer

Nucleotides written in CAPITAL LETTERS correspond to VEGF promoter sequence -267 to 0.  
Nucleotides written in small letters correspond to VEGF gene sequence +1 to+50.

A sequence in dark green was used as a synthetic oligo for SP1 EMSA experiments

A sequence in light green was used as a synthetic oligo for SP4 EMSA experiments. Mutated SP4 sequence is written in small blue letters.

**Fig. S1 Effect of SP4 on VEGF-mediated tube formation by human dermal microvascular**

**endothelial cells (HDMEC).** Cells were transiently transfected with either SP4 siRNA or

scrambled (Scramb) siRNA, and stimulated for 16 hrs with conditioned medium (10% v/v)

from HPMC treated without or with IL-6+sIL-6R (both at 100 ng/ml) for 24 hours. \*P<0.05 vs.

cells stimulated with IL-6+sIL-6R in the absence of siRNA, n=4. Representative phase contrast

images (magnification 100 x)

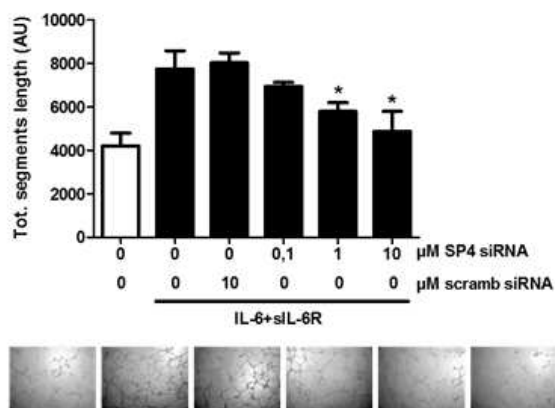


**Fig. S2 Effect of IL-6 signaling in mice on peritoneal vasculature following repeated peritonitis.** WT and IL-6<sup>-/-</sup> mice received 4 consecutive doses of SES (i.p.) administered at 7-day intervals. Histological evaluation was recorded on day-49 post first SES challenge.

Sections were stained for either PECAM-1 (CD31) (A, B) or podoplanin (C, D). Representative 40x magnification (insert panels: 400x magnification) fields are shown. Scores displayed in Panels B and D reflect digital assessments of immunohistochemistry staining as described in Materials and Methods.

Formatted: Not Highlight

Deleted: fields are shown

Deleted: ?

Formatted: Not Highlight

Formatted: Not Highlight

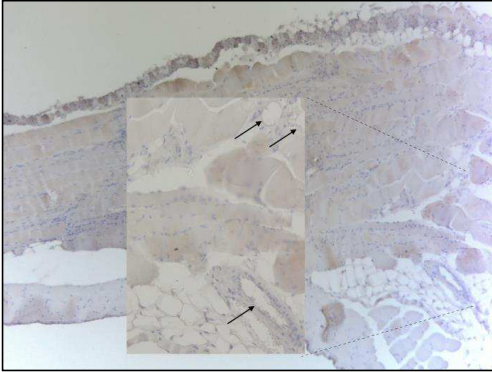
Deleted: Magnification and/or further details ? ¶  
How were the scores calculated? (B and D)¶

Formatted: Not Highlight

Formatted: Not Highlight

**A**

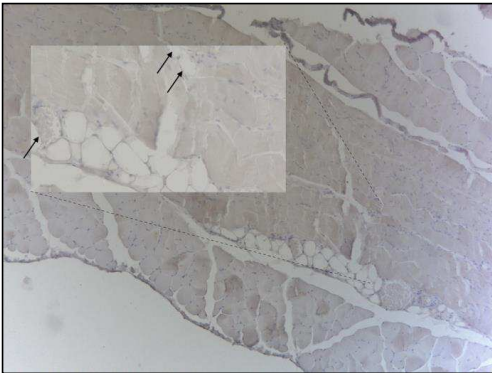
WT 4xSES d49 Isotype Control



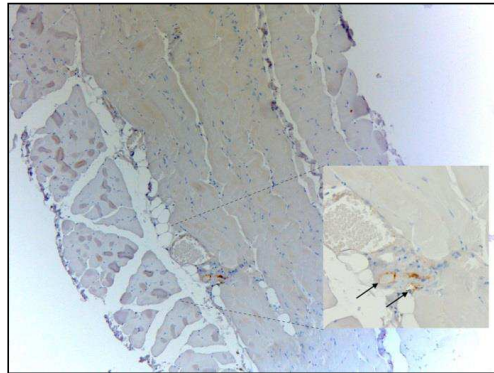
WT 4xSES d49 CD31



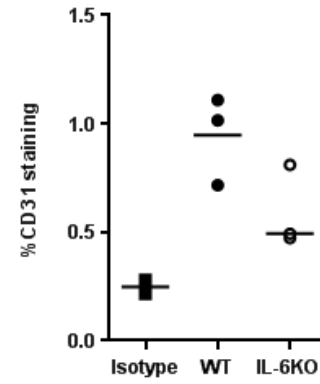
*Il6*<sup>-/-</sup> 4xSES d49 Isotype Control



*Il6*<sup>-/-</sup> 4xSES d49 CD31

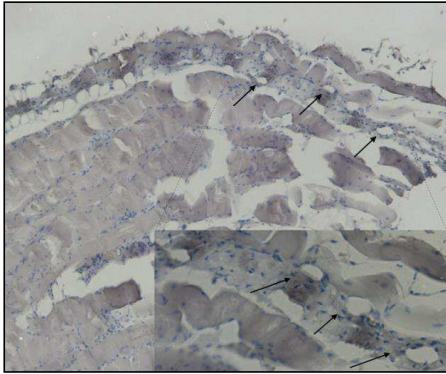


**B**

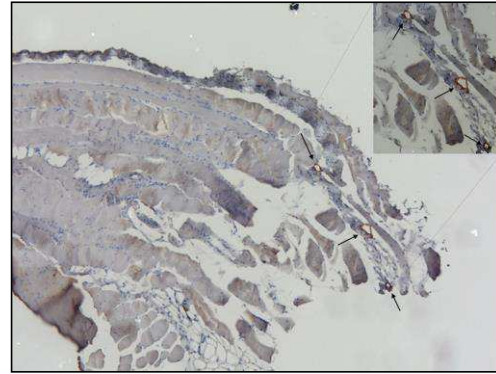


C

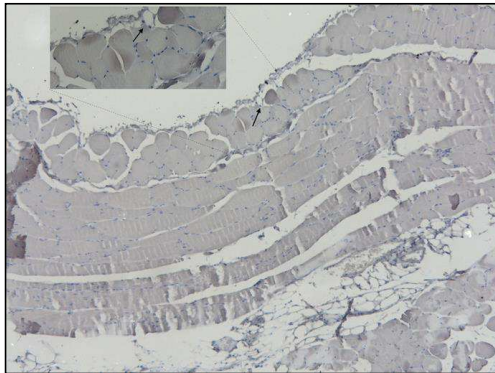
WT 4xSES d49 Isotype Control



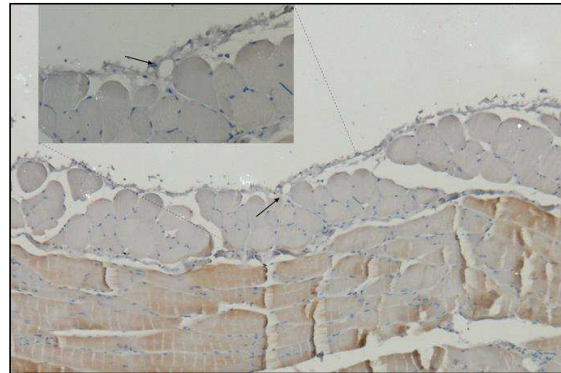
WT 4xSES d49 CD31



*Il6*<sup>-/-</sup> 4xSES d49 Isotype control



*Il6*<sup>-/-</sup> 4xSES d49 Pdpn



D

